The Astrophysical Journal, 658:1069–1080, 2007 April 1

ON PARTICLE ACCELERATION AROUND SHOCKS. III. SHOCK WAVES MOVING AT ARBITRARY SPEED. THE CASE OF LARGE-SCALE MAGNETIC FIELD AND ANISOTROPIC SCATTERING

G. Morlino
Dipartimento di Fisica, Università di Pisa, Pisa, Italy

P. Blasi
INAF/Osservatorio Astronomico di Arcetri, Firenze, Italy

and

M. Vietri
Scuola Normale Superiore, Pisa, Italy
Received 2005 December 11; accepted 2006 December 20

ABSTRACT

A mathematical approach to investigate particle acceleration at shock waves moving at arbitrary speed in a medium with arbitrary scattering properties was first discussed in work by Vietri and Blasi. We use this method and somewhat extend it in order to include the effect of a large-scale magnetic field in the upstream plasma, with arbitrary orientation with respect to the direction of motion of the shock. We also use this approach to investigate the effects of anisotropic scattering on spectra and anisotropies of the distribution function of the accelerated particles.

Subject headings: cosmic rays — shock waves

1. INTRODUCTION

The theory of particle acceleration at shock fronts moving with arbitrary speeds (from Newtonian to ultrarelativistic) can be formulated in a simple and exact form (Vietri 2003; Freiling et al. 2003) at least in the so-called test particle limit, which neglects the dynamical reaction of accelerated particles on the shock. In this framework, all the basic physical ingredients can be taken into account in an exact way, with special reference to the type of scattering that is responsible for the particles returning to the shock front from the upstream and downstream plasmas. The information about scattering is introduced in the problem through the function $w(\mu, \mu')$, which expresses the probability per unit length that a particle moving in the direction μ' is scattered to a new direction μ. It is worth stressing that w can have a different functional form in the upstream and downstream plasmas, in particular, in the case of relativistic shocks.

The repeated scatterings of the particles lead eventually to a return to the shock front, as described in terms of the conditional probability $P_u(\mu_0, \mu)$ [$P_d(\mu_0, \mu)$] that a particle entering the upstream (downstream) plasma in the direction μ_0 returns to the shock and crosses it in the direction of the downstream (upstream) plasma, μ. The mathematical method adopted to calculate the two very important functions P_u and P_d based on the knowledge of the elementary scattering function w was described in detail in Blasi & Vietri (2005) and is based on solving two nonlinear integral-differential equations in the two independent coordinates μ_0 and μ.

Vietri (2003) showed on very general grounds that the spectrum of accelerated particles is a power law for all momenta exceeding the injection momentum. The slope of such a power law and the anisotropy pattern of the accelerated particles near the shock front are fully determined by the conditional probabilities P_d and P_u and by the equation of state of the downstream plasma. Particle acceleration at shock fronts has been previously investigated through different methods, both semianalytical (see, e.g., Kirk & Schneider 1987; Gallant & Achterberg 1999; Kirk et al. 2000; Achterberg et al. 2001) and numerical, by using Monte Carlo simulations (e.g., Bednard & Ostrowski 1998; Lemoine & Pelletier 2003; Niemiec & Ostrowski 2004; Lemoine & Revenu 2006). The theory of particle acceleration developed by Vietri (2003) and Blasi & Vietri (2005) has been checked versus several of these calculations existing in the literature, both in the case of nonrelativistic shocks and for relativistic shocks, and assuming small as well as large pitch angle isotropic scattering (see Blasi & Vietri [2005] for an extensive discussion of these results).

In this paper we extend the application of this new theoretical framework to two new interesting situations: (1) the presence of a coherent large-scale magnetic field in the upstream fluid and (2) anisotropic scattering. In both cases we calculate the spectrum of accelerated particles and the distribution in pitch angle (upstream and downstream) for shock fronts moving with arbitrary velocity. The results of point (1) are compared with those obtained in Achterberg et al. (2001) that were carried out for a parallel ultrarelativistic shock.

The paper has been inspired by the need to address several points of phenomenological relevance. As far as relativistic shocks are concerned, it was understood that the return of the particles to the shock surface from the upstream region can be warranted even in the absence of scattering, provided the background magnetic field is at an angle with the shock normal (e.g., Achterberg et al. 2001). This is due to the fact that the shock and the accelerated particles remain spatially close and regular deflection takes place before particles can experience the complex, possibly turbulent structure of the upstream magnetic field. This implies that the calculation of the spectrum of the accelerated particles cannot be calculated using a formalism based on the assumption of pitch angle diffusion, as in the vast majority of the existing literature.

In the downstream region, the motion of the shock is always quasi-Newtonian, even when the shock moves at ultrarelativistic speeds. This implies that the propagation of the particles is generally well described by (small or large) pitch angle scattering. However, the turbulent structure of the magnetic field responsible for the scattering is likely to have an anisotropic structure and to therefore be responsible for anisotropic scattering. In fact, even

in the case of isotropic turbulence, the scattering can determine an anisotropic pattern of particle scattering. It follows that a determination of the spectrum able to take into account these potentially important situations is very important.

The outline of the paper is as follows. In § 2 we briefly summarize the theoretical framework introduced in Vietri (2003) and Blasi & Vietri (2005). In § 3 we consider in detail the case of a large-scale magnetic field in the upstream frame and no scattering of the particles. The scattering is assumed to be isotropic in the downstream plasma. In § 4 we introduce the possibility of anisotropic scattering in both upstream and downstream plasmas. We summarize in § 5.

2. AN EXACT SOLUTION FOR THE ACCELERATED PARTICLES IN ARBITRARY CONDITIONS: A SUMMARY

In this section we summarize the main characteristics of the theory of particle acceleration developed by Vietri (2003) and Blasi & Vietri (2005). The reader is referred to this previous work for further details. The power of this novel approach is in its generality: it provides an exact solution for the spectrum of the accelerated particles and at the same time the distribution in pitch angle that the particles acquire due to scattering in the upstream and downstream fluids. This mathematical approach is applicable without restrictions on the velocity of the fluid speeds (from Newtonian to ultrarelativistic) and irrespective of the scattering properties of the background plasmas (small as well as large angle scattering, isotropic or anisotropic scattering). The only condition that is necessary for the theory to work is common to most if not all other semianalytical approaches existing in the literature, namely, that the acceleration must take place in the test particle regime; no dynamical reaction is currently introduced in the calculations. As a consequence, the shock is assumed to conserve its strength during the acceleration time, and the acceleration is assumed to have reached a stationary regime.

The directions of motion of the particles in the downstream and upstream frames are identified through the cosine of their pitch angles, all evaluated in the comoving frames of the fluids that they refer to. The direction of motion of the shock, identified as the z-axis, is assumed to be oriented from upstream to downstream, following the direction of motion of the fluid in the shock frame ($\mu = 1$ corresponds to particles moving toward the downstream section).

The transport equation for the particle distribution function g, as obtained in Vietri (2003), in a relativistically covariant derivation reads

$$\gamma(u+\mu)\frac{\partial g}{\partial z} = \int\int \{[-W(\mu',\mu,\phi',\phi)g(\mu,\phi) + W(\mu,\mu',\phi,\phi')g(\mu',\phi')]d\mu'\,d\phi'\} + \omega\frac{\partial g}{\partial \tilde{\phi}}, \quad (1)$$

in which both scattering and regular deflection in a large-scale magnetic field are taken into account.

Here all quantities are written in the fluid frame, with the exception of the spatial coordinate z, the distance from the shock along the shock normal, which is measured in the shock frame. The variables u and γ are, respectively, the velocity and the Lorentz factor of the fluid with respect to the shock, and θ and ϕ are the polar coordinates of particles in momentum space, measured with respect to the shock normal, while $\tilde{\phi}$ is the longitudinal angle around the magnetic field direction. As usual, $\mu = \cos\theta$ and $\omega = eB/E$ is the particle Larmor frequency. The function $W(\mu,\mu',\phi,\phi')$ is the scattering probability per unit length, namely, the probability that a particle moving in the direction (μ',ϕ') is scattered to a direction (μ,ϕ) after traveling a unit length.

An important simplification of equation (1) occurs when an axial symmetry is assumed. In this case, the scattering probability depends only on $\Delta \equiv \phi - \phi'$, and the large-scale magnetic field can be either zero or different from zero but parallel to the shock normal. In both cases, it is straightforward to integrate equation (1) over ϕ: the two-dimensional integral on the right-hand side simplifies to an integral in one dimension, while the term $\omega(\partial g/\partial\tilde{\phi})$ disappears.

These simplifications lead to

$$\gamma(u+\mu)\frac{\partial g}{\partial z} = \int [-w(\mu',\mu)g(\mu) + w(\mu,\mu')g(\mu')]\,d\mu', \quad (2)$$

where

$$w(\mu,\mu') \equiv \int W(\mu,\mu',\Delta)\,d\Delta,$$
$$g(\mu) \equiv \frac{1}{2\pi}\int g(\mu,\phi)\,d\phi.$$

The physical ingredients are all contained in the two conditional probabilities $P_u(\mu_0,\mu)$ and $P_d(\mu_0,\mu)$; these two functions provide, respectively, the probability that a particle entering the upstream and downstream plasma along a direction μ_0 exits it along a direction μ. In the absence of large-scale coherent magnetic fields, the two functions $P_u(\mu_0,\mu)$ and $P_d(\mu_0,\mu)$ were defined through a set of two integral-differential nonlinear equations by Blasi & Vietri (2005). We report these equations here for completeness:

$$P_u(\mu_0,\mu)\left[\frac{d(\mu_0)}{u+\mu_0} - \frac{d(\mu)}{u+\mu}\right] = \frac{w(\mu,\mu_0)}{u+\mu_0} - \int_{-u}^{1} d\mu'\,\frac{w(\mu,\mu')P_u(\mu_0,\mu')}{u+\mu'} + \int_{-1}^{-u} d\mu'\,\frac{w(\mu',\mu_0)P_u(\mu',\mu)}{u+\mu_0} - \int_{-1}^{-u} d\mu'\,P_u(\mu',\mu)\int_{-u}^{1} d\mu''\,\frac{w(\mu',\mu'')P_u(\mu_0,\mu'')}{u+\mu''}, \quad (3)$$

$$P_d(\mu_0,\mu)\left[\frac{d(\mu_0)}{u+\mu_0} - \frac{d(\mu)}{u+\mu}\right] = \frac{w(\mu,\mu_0)}{u+\mu_0} + \int_{-u}^{1} d\mu'\,\frac{P_d(\mu',\mu)w(\mu',\mu_0)}{u+\mu_0} - \int_{-1}^{-u} d\mu'\,\frac{P_d(\mu_0,\mu')w(\mu,\mu')}{u+\mu'} - \int_{-u}^{1} d\mu'\,P_d(\mu',\mu)\int_{-1}^{-u} d\mu''\,\frac{w(\mu',\mu'')P_d(\mu_0,\mu'')}{u+\mu''}, \quad (4)$$

where

$$d(\mu) \equiv \int_{-1}^{+1} w(\mu',\mu)\,d\mu', \quad (5)$$

which is unity by definition.

It is worth stressing that equation (3) automatically provides the correct normalization for the return probability from upstream, $\int_{-u}^{1} d\mu' P_u(\mu_0,\mu') = 1$, independent of the entrance angle μ_0. In § 3 we generalize the method to include the possibility of deflection by large-scale magnetic fields, which is one of the achievements of this work. In that case we show that the return probability

from upstream is no longer bound to be unity due to the escape of particles from the upstream region.

The procedure for the calculation of the slope of the spectrum of accelerated particles, as found by Vietri (2003) and Blasi & Vietri (2005), is as follows. For a given Lorentz factor of the shock (γ_s), the velocity of the upstream fluid $u = \beta_s$ is calculated. The velocity u_d of the downstream fluid is found from the usual jump conditions at the shock and through the adoption of an equation of state for the downstream fluid.

Once the two functions P_u and P_d have been calculated, the slope of the spectrum, as discussed in Vietri (2003), is given by the solution of the integral equation

$$(u_d + \mu)g(\mu) = \int_{-u_d}^{1} d\xi\, Q^T(\xi, \mu)(u_d + \xi)g(\xi), \qquad (6)$$

where

$$Q^T(\xi, \mu) = \int_{-1}^{-u_d} d\nu\, P_u(\nu, \mu)P_d(\xi, \nu)\left(\frac{1 - u_{\rm rel}\mu}{1 - u_{\rm rel}\nu}\right)^{3-s}, \qquad (7)$$

$u_{\rm rel} = (u - u_d)/(1 - uu_d)$ is the relative velocity between the upstream and downstream fluids, and $g(\mu)$ is the angular part of the distribution function of the accelerated particles, which contains all the information about the anisotropy. Note that in equation (7) all variables and functions are evaluated in the downstream frame, while the P_u calculated through equation (3) is in the frame comoving with the (upstream) fluid. The P_u that needs to be used in equation (7) is therefore

$$P_u(\nu, \mu) = P_u(\tilde{\nu}, \tilde{\mu})\frac{d\tilde{\mu}}{d\mu} = P_u(\tilde{\nu}, \tilde{\mu})\left[\frac{1 - u_{\rm rel}^2}{(1 - u_{\rm rel}\mu)^2}\right].$$

The solution for the slope s of the spectrum is found by solving equation (6). In general, this equation has no solution except for one value of s. Finding this value provides not only the slope of the spectrum but also the angular distribution function $g(\mu)$.

2.1. *The Special Case of Isotropic Scattering*

No assumption has been introduced so far about the scattering processes that determine the motion of the particles in the upstream and downstream plasmas, with the exception of the axial symmetry of the function $W(\mu, \mu', \phi, \phi')$. A special case of this symmetric situation is that of isotropic scattering, which takes place when the scattering probability W only depends on the deflection angle Θ, which is related to the initial and final directions through

$$\cos\Theta \equiv \mu\mu' + \sqrt{1 - \mu^2}\sqrt{1 - \mu'^2}\cos(\phi - \phi'). \qquad (8)$$

Among the many functional forms that correspond physically to isotropic scattering, the simplest one is

$$W(\mu, \mu', \phi, \phi') = W(\cos\Theta) = \frac{1}{\sigma}e^{-(1-\cos\Theta)/\sigma}, \qquad (9)$$

where σ is the mean scattering angle. Integration of equation (9) over $\phi - \phi'$ leads to

$$w(\mu, \mu') = \frac{1}{\sigma}e^{-(1-\mu\mu')/\sigma}I_0\left(\frac{\sqrt{1 - \mu^2}\sqrt{1 - \mu'^2}}{\sigma}\right), \qquad (10)$$

where $I_0(x)$ is the Bessel function of order 0. Equation (9), first introduced in Blasi & Vietri (2005), naturally satisfies the requirement of being symmetric under rotations around the normal to the shock surface. In the limit $\sigma \ll 1$, this function becomes a Dirac delta function, strongly peaked around the forward direction, corresponding to isotropic small pitch angle scattering (SPAS). For the opposite limit, that is $\sigma \gg 1$, w becomes flat and corresponds to the case of isotropic large angle scattering (LAS). In § 4.1 we modify this functional form to introduce the possibility of anisotropic scattering.

3. DEFLECTION BY A REGULAR MAGNETIC FIELD IN THE UPSTREAM REGION

It is well known that particle acceleration at a shock front with a parallel magnetic field without scattering centers does not work. This magnetic scattering may be self-generated by the same particles, but the process of generation depends on the conditions in specific astrophysical environments. The case in which a regular magnetic field not parallel to the shock normal is present in the upstream fluid is quite interesting in that it allows for the return of the particles to the shock front even in the absence of scattering. In this section we investigate in detail the process of acceleration at shocks with arbitrary velocity when only a regular large-scale magnetic field is present upstream (no scattering). We assume that enough turbulence is instead present in the downstream plasma to guarantee magnetic scattering of the particles.

There are two main differences introduced by this situation when compared with the standard case considered in § 2:

Particle motion in the upstream region is deterministic.—The stochasticity introduced by the interaction with scattering centers is assumed to be absent. This requires a new determination of the return probability P_u introduced above.

The presence of regular magnetic field with arbitrary orientation breaks the axial symmetry around the shock normal.—This, in principle, would force us to treat the problem in the four angular variables μ_0, ϕ_0, μ, and ϕ.

In the following sections we show how addressing the first point in fact solves the second point as well.

3.1. *Upstream Return Probability*

Let us consider a particle entering upstream in the direction identified by the two angles μ_0 and ϕ_0 and returning to the shock along the direction identified by μ and ϕ. Since the motion of the particle is deterministic, the return direction is completely defined by the incoming coordinates, and we can write in full generality

$$P_u(\mu_0, \phi_0; \mu, \phi) = (2\pi)^{-1}\delta(\mu - \mu_1(\mu_0, \phi_0)) \times \delta(\phi - \phi_1(\mu_0, \phi_0)), \qquad (11)$$

where μ_1 and ϕ_1 are obtained from the solution of the equation of motion, as discussed below. One can see that P_u is effectively a function of only two variables.

In order to apply the same mathematical procedure introduced in § 2, we need to write P_u as a function of azimuthal angles only. Therefore, we use the properties of the delta function in $\delta(\mu - \mu_1(\mu_0, \phi_0))$ to write

$$P_u(\mu_0, \phi_0; \mu, \phi) = \frac{1}{2\pi}\left|\frac{\partial\phi_0(\mu_0, \mu)}{\partial\mu}\right|\delta\left(\phi_0 - \bar{\phi}_0\right)\delta(\phi - \phi_1) \equiv P_u(\mu_0, \mu)\,\delta\left(\phi_0 - \bar{\phi}_0\right)\delta(\phi - \phi_1). \qquad (12)$$

We now show that $P_u(\mu_0, \mu)$, as defined by equation (12), is exactly the function to be used in equation (7). This is easily shown

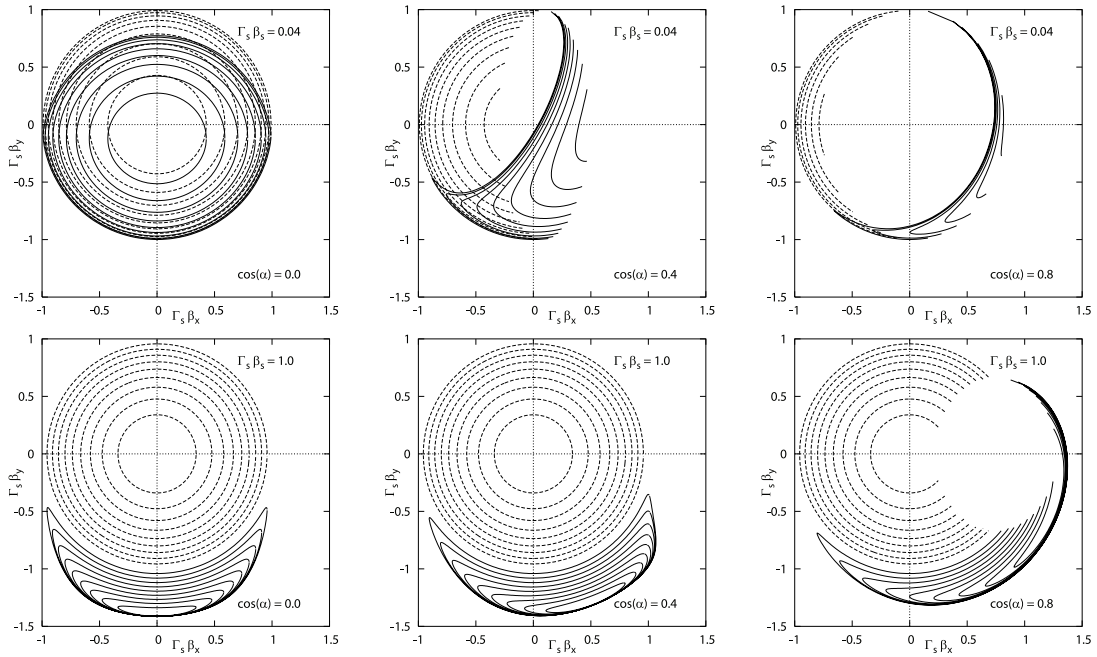

FIG. 1.—Location of the particles entering the upstream region (*dashed lines*) and returning to the downstream region (*solid lines*) after being deflected by the magnetic field upstream. The directions are plotted in the plane $\Gamma_s\beta_{p,x}$-$\Gamma_s\beta_{p,y}$, where $\beta_{p,x}$ and $\beta_{p,y}$ are the components of the particle velocity along the *x*- and the *y*-axis, respectively. The origin corresponds to particles entering along the shock normal. Circles correspond to particles having constant μ_0. The top row refers to $\Gamma_s\beta_s = 0.04$. The bottom row refers to $\Gamma_s\beta_s = 1.0$. In both cases we show the effects of three different orientations of the magnetic field (*from left to right*: $\cos\alpha = 0.0$, 0.4, and 0.8). The presence of an empty region when $\cos\alpha > \beta_s$ is due to particle leakage from upstream. (Compare with Fig. 1 in Achterberg et al. [2001].)

by writing the fluxes of particles ingoing to and outgoing from the upstream plasma,

$$J_+(\mu,\phi) = \int_{-1}^{-u} d\mu' \int_0^{2\pi} d\phi' P_u(\mu',\phi',\mu,\phi) J_-(\mu',\phi'), \quad (13)$$

which, when integrated over ϕ, yields

$$J_+(\mu) \equiv \int d\phi J_+(\mu,\phi) = \int_{-1}^{-u} d\mu' P_u(\mu',\mu) J_-(\mu'), \quad (14)$$

where we assumed that J_- is independent of ϕ. This is exactly the same relationship as was used in Vietri (2003) and proves our point that the system may, on average, still be treated as if it were symmetric about the shock normal.

The key assumption here is that the flux crossing back into the upstream region from the downstream one, J_-, be independent of the azimuthal angle ϕ. This is of course true in the Newtonian regime, because there the residence time for all particles diverges, and there is time for deflections to effectively erase anisotropies in the ϕ-direction. But this must be true a fortiori in the relativistic regime, when one considers that the properties of scattering are of course still the same as in the Newtonian regime, while the surface to be recrossed, i.e., the shock, is running away from the particles at a speed that becomes, asymptotically, a fair fraction of the particles' speed. So, while not exactly true, the independence of J_- from ϕ is at least a good approximation.

In order to write $P_u(\mu_0,\mu)$ in a more explicit way, we need to solve the equation of motion of the particles, namely, find the direction in which the particles recross the shock front as a function of the incoming direction. Particles move following a helicoidal trajectory around the magnetic field direction, indicated here as $\tilde{z}$. The problem is simplest if expressed in the frame $\tilde{O}$ comoving with the upstream fluid but with the polar axis coincident with $\tilde{z}$. We mark with a tilde all quantities expressed in this frame. The equations of motion in the frame $\tilde{O}$ are

$$\tilde{\mu}(t) = \tilde{\mu}_0, \quad (15)$$

$$\tilde{\phi}(t) = \tilde{\phi}_0 + \omega t, \quad (16)$$

where t is time and ω is the Larmor frequency. The particles recross the shock when $z_{\rm particle}(t) = z_{\rm shock}(t)$. This condition expressed in the frame $\tilde{O}$ reads

$$\sin(\omega t + \tilde{\phi}_0) - \sin\tilde{\phi}_0 = \frac{\tilde{\mu}_0\cos\alpha + \beta_s}{\sin\alpha\sin\tilde{\theta}_0}\omega t, \quad (17)$$

where α is the angle between the shock normal z and the magnetic field direction $\tilde{z}$. The solution of equation (17) gives the upstream residence time t^* of the particles, which is to be evaluated numerically.

The angles that identify the recrossing direction, as functions of the residence time, are

$$\tilde{\mu}_1 = \tilde{\mu}_0, \quad (18)$$

$$\tilde{\phi}_1 = \tilde{\phi}_0 + \omega t^*(\tilde{\mu}_0,\tilde{\phi}_0). \quad (19)$$

A rotation by the angle α provides us with the recrossing coordinates μ_1 and ϕ_1 in the fluid frame. At this point, the Jacobian in equation (12) can be calculated, although some care is needed because this Jacobian is not a single valued function; for each pair (μ_0,μ), the Jacobian has two values. This degeneracy arises because of the substitution of ϕ_0 with μ, since each μ corresponds in general to two possible values of ϕ_0. This is clear from Figure 1, where we show some examples of solutions; the directions of entrance and escape from the upstream fluid are plotted for different values of the shock speed and for different orientations of the large-scale magnetic field.

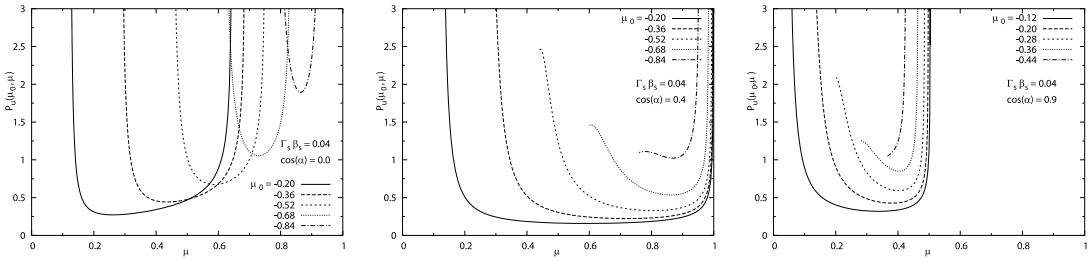

FIG. 2.—Conditional probability $P_u(\mu_0, \mu)$ as a function of the outgoing direction μ, for a fixed value of the shock speed ($\Gamma_s\beta_s = 0.04$) with three different inclinations of the magnetic field ($\cos\alpha = 0.0$, 0.4, and 0.9). For each plot the different lines correspond to different values of the ingoing direction μ_0.

Equation (17) admits a solution $t^* > 0$ only if the two following conditions are fulfilled.

1. The initial velocity of a particle along the shock normal must be larger than the shock speed (otherwise the particle is prevented from crossing the shock to start with). This implies

$$\mu_0 < -\beta_s. \tag{20}$$

2. The particle velocity along the shock normal has to be less than the shock speed, namely,

$$\tilde{\mu}_0 \cos\alpha > -\beta_s. \tag{21}$$

Particles not satisfying this last condition escape the shock region toward upstream infinity, a situation that is not realized in the case of scattering considered in § 2. This escape process occurs only for $\cos\alpha > -\beta_s$ and results in the loss of particles having the entrance pitch angles cosine exceeding $\mu_{\min}(\mu_0, \phi_0)$. In fact for $\cos\alpha < -\beta_s$, $\mu_{\min} = \text{const} = -1$ and all particles eventually recross the shock. When the particles are allowed to escape upstream, the acceleration is clearly expected to become less efficient and give rise to softer spectra of the accelerated particles (see § 3.2).

Putting together all of the above, we can finally write the upstream conditional probability as

$$P_u(\mu_0, \mu) = \frac{1}{2\pi} \sum_{i=1,2} \left| \frac{\partial\phi_0}{\partial\mu} \right|_i \theta(-\mu_0 - \beta_s)\, \theta(\mu_0 - \mu_{\min}(\mu_0, \mu)), \tag{22}$$

where the sum is extended over the two branches of the Jacobian.

For $\cos\alpha < -\beta_s$, the particles always return to the shock front, and this forces the return probability to be unity when integrated over all outgoing directions,

$$\int_{-u}^{1} d\mu\, P_u(\mu_0, \mu) = 1. \tag{23}$$

This integral condition is trivially satisfied by equation (22) and is used as a check for P_u after its numerical computation.

Figures 2, 3, and 4 show some examples of our calculations of $P_u(\mu_0, \mu)$ as a function of μ for different values of μ_0, for a Newtonian, a transrelativistic, and a relativistic shock, respectively. For each case we show the results for different inclinations of the magnetic field with respect to the shock normal. It is worth noticing that P_u does not change significantly when the inclination of the magnetic field varies in the range $0 < \cos\alpha < \beta_s$ at a given shock speed. Therefore, we do not expect a significant variation of the spectral slope in this range. In § 3.2 we show that this is in fact the case.

3.2. *Spectrum and Anisotropy of the Accelerated Particles for a Large-Scale Magnetic Field Upstream*

In this section we use equations (6) and (7) to calculate the spectrum and angular distribution of the accelerated particles at the shock front. The return probabilities are calculated assuming that in the downstream fluid there is isotropic scattering, so that P_d can be calculated from equation (4) using equation (10) as a scattering function. We assume $\sigma = 0.01$ for the SPAS regime and $\sigma = 10$ for the LAS regime. In the upstream fluid we assume that particles can only be deflected by a large-scale coherent magnetic field with arbitrary orientation with respect to the normal to the shock front. The return probability P_u is therefore calculated as discussed in detail in § 3.1.

The only information still lacking to proceed further is an equation of state for the medium that would allow us to compute the velocity of the downstream fluid from the jump conditions at the shock front (see, e.g., Gallant 2002). We assume that the gas upstream has zero pressure. Moreover, in the following we assume everywhere that the magnetic field has no dynamical role, so that the standard jump conditions for an unmagnetized shock can be adopted (the role of the magnetic field becomes important when the magnetic energy density becomes comparable with the thermal energy density [Kirk & Duffy 1999]).

Following much of the previous literature, we adopt the Synge equation of state for the downstream gas (Synge 1957), assuming that only protons contribute. Although used widely, this assumption may not be well justified in a general case. We will illustrate our conclusions on the role of the equation of state for

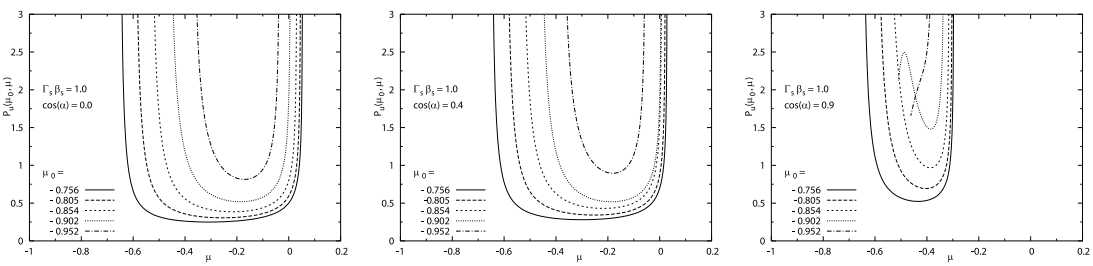

FIG. 3.—Same as Fig. 2, but for a transrelativistic shock ($\Gamma_s\beta_s = 1.0$, $\beta_s = 0.707$).

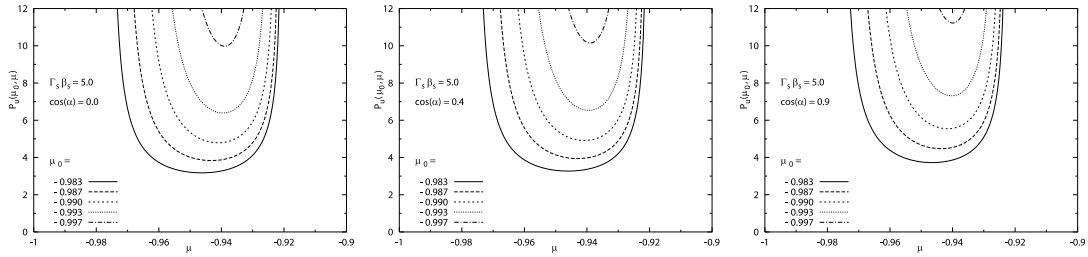

FIG. 4.—Same as Fig. 2, but for a relativistic shock ($\Gamma_s\beta_s = 5.0$, $\beta_s = 0.98$). The three plots are very similar to each other because the condition $\cos\alpha > \beta_s$ is never reached.

the spectrum and anisotropy of the accelerated particles in a separate paper.

Within this set of assumptions, it is worth reminding that the compression ratio $u_{\rm up}/u_{\rm down}$ tends asymptotically to 4 for a nonrelativistic shock (even for shock speeds that are known to give lower compression factors) and to 3 for ultrarelativistic shocks.

The simplest case to consider is that of a shock in which the large-scale coherent magnetic field in the upstream region is parallel to the shock front ($\cos\alpha = 0$). This is known as a perpendicular shock. The angular distribution and the slope of the spectrum of the accelerated particles are plotted in Figure 5 (the LAS [SPAS] case is shown in the left [right] panel) and Figure 6, respectively, for various shock velocities ranging from Newtonian to relativistic.

The angular distribution of the particles in the downstream frame is seen to be rather anisotropic for the SPAS case, even in the Newtonian regime. LAS is evidently more efficient in isotropizing the accelerated particles. The anisotropies do not seem to affect the spectrum of the accelerated particles in the case of nonrelativistic shocks: the slope of the spectrum for both SPAS and LAS is 4.000 ± 0.001. The effect becomes more prominent for faster shocks and in particular for relativistic shocks. In the SPAS case, for $\Gamma_s\beta_s = 10$ we found $s = 4.272 \pm 0.001$, compatible with $s = 4.28 \pm 0.01$, obtained by Achterberg et al. (2001) for $\Gamma_s = 10$ with a Monte Carlo simulation.

In Figure 6, the dotted and dashed lines refer to the SPAS and LAS cases, respectively. At first glance, it may appear rather surprising that in the limit of relativistic shocks the spectrum of accelerated particles is softer in the LAS regime than it is in the SPAS regime, since LAS is envisioned as more efficient in redirecting the particles to the shock front. This intuitive vision turns out to be incorrect, as also shown in Table 1, where we list the slope, the average energy gain, and the return probability from downstream (as defined in eqs. [26] and [29]) for a relativistic shock with $\Gamma_s\beta_s = 5.0$.

One can see that while the average energy gain is similar in the two cases, the return probability in the case of LAS is 20% lower than for the SPAS case. Qualitatively this can be understood as follows. When the shock velocity increases, particles are caught up to by the shock front when they have traveled only a small fraction (of order $1/\Gamma_s$) of their gyration. Once downstream, LAS is likely to swing them far from the shock front in a few interactions, while SPAS deflects their trajectories rather slowly, yet they remain in the vicinity of the shock surface. This is responsible for the 20% difference in the average return probabilities in the two cases. This is also shown in Figure 7, where we plot the particle flux $J(\mu) \equiv |\mu + u_d| g(\mu)$ in terms of downstream coordinates. The total flux of particles entering the downstream section ($-u_d < \mu < 1$) is normalized to unity. It is clear from Figure 7 that the flux of particles returning to the shock is slightly larger for the case of SPAS (*dashed line in the range* $-1 < \mu < -u_d$).

A more interesting question concerns the effect of the orientation of the large-scale magnetic field with respect to the normal to the shock. We have already emphasized that for any orientation different from that of a perpendicular shock, and in the absence of scattering processes upstream, particles are lost from the upstream region, because the shock cannot catch up with their motion. This happens when $\cos\alpha > -\beta_s$, so that the phenomenon

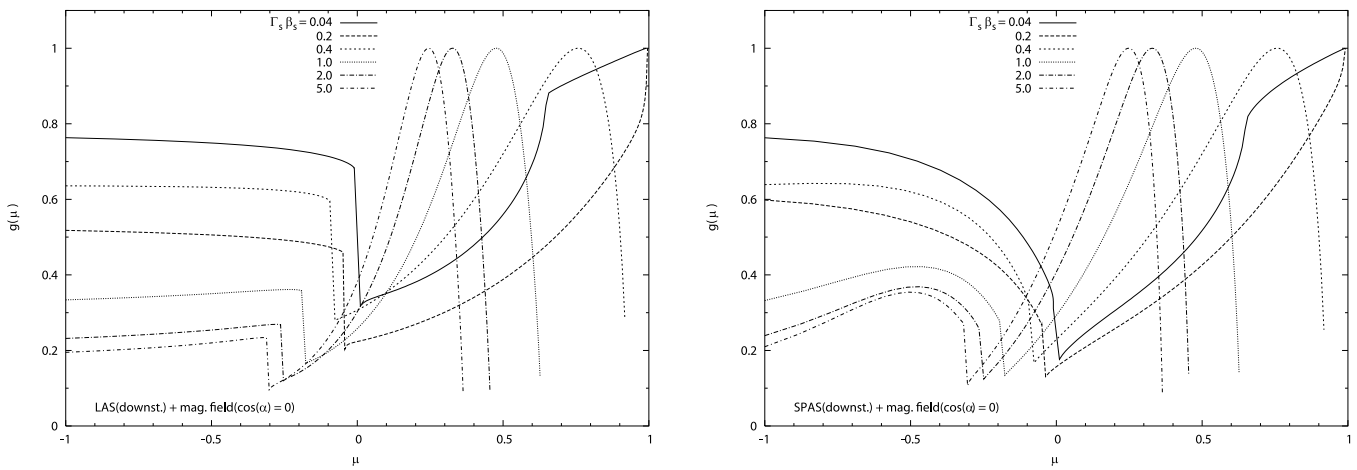

FIG. 5.—Particle distribution function at the shock front when a large-scale coherent magnetic field is present in the upstream region, with a direction parallel to the shock plane. In the downstream region particles are scattered in the LAS (*left*) or in the SPAS regime [*right*; here the maximum of $g(\mu)$ is arbitrarily set equal to 1]. Several values of shock speeds are shown. The particle distribution functions always show a jump at $\mu = -\beta_s$. Large angle scattering makes distribution functions flatter compared with the small angle scattering case for $-1 < \mu < -u_d$.

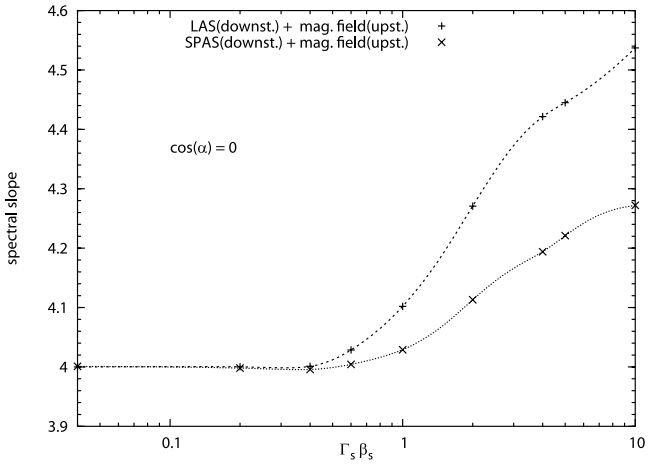

FIG. 6.—Spectral index vs. shock speed for the same configuration as in Fig. 5.

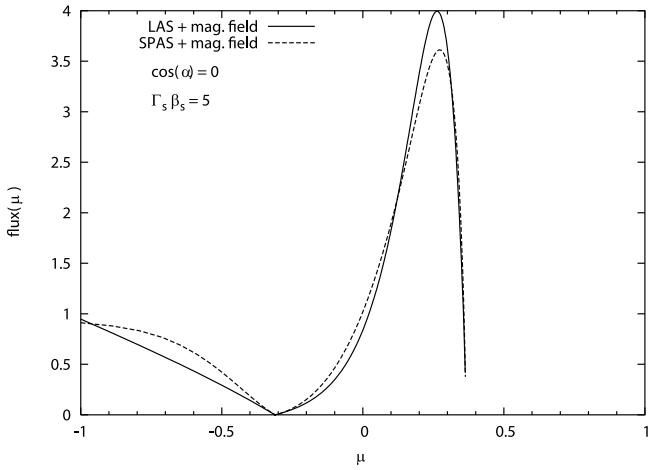

FIG. 7.—Particle flux $J(\mu) \equiv |\mu + u_d| g(\mu)$ across the shock front, as it appears in the downstream frame, when the upstream magnetic field is parallel to the shock ($\cos \alpha = 0$) and the downstream fluid is in the LAS regime (*solid line*) or SPAS regime (*dashed line*). The shock speed is $\Gamma_s \beta_s = 5.0$. The flux entering downstream (i.e., for $-u_d < \mu < 1$) is normalized to 1. In this way we see that downstream return probability, i.e., the integrated flux for $-1 < \mu < -u_d$, is larger when the downstream region is in the SPAS regime.

is increasingly more important for shocks approaching the parallel configuration. This is reflected in increasingly softer spectra. In the limit $\cos \alpha \rightarrow 1$, all particles escape from the upstream region, and no acceleration takes place.

The slope of the spectrum as obtained from our calculations is plotted in Figure 8 (*solid lines and symbols*) as a function of $\cos \alpha$ for three different shock speeds ($\Gamma_s \beta_s = 0.6$, 1.0, and 2.0). When there is no particle escape, the slope s is actually a constant, while it increases dramatically (and in fact diverges, showing the disappearance of the acceleration process) for values of $\cos \alpha$ larger than $-\beta_s$. In Figure 8 (*inset*) we also plot the return probability from upstream. For very inclined shocks the return probability is still very close to unity, as in the case of upstream scattering, but it drops rapidly for increasingly less inclined shocks.

The steepening of the spectrum due to leakage of the particles toward upstream infinity can also be understood in terms of a Bell-like (Bell 1978) calculation, when carried out for the case of a large-scale coherent magnetic field. The slope of the spectrum is related to the average return probability and the average energy gain of the particles per cycle back and forth through the shock front through the expression

$$s = 3 - \frac{\log \langle P_{\rm ret} \rangle}{\log \langle G \rangle}, \tag{24}$$

where $\langle G \rangle$ is the mean amplification in a single cycle (downstream $\rightarrow$ upstream $\rightarrow$ downstream) and $\langle P_{\rm ret} \rangle$ is the mean probability of returning to the shock. One should keep in mind that Bell's method, as expressed through the equation above, is flawed in that it does not take into proper consideration the correlation between the amplification factor and the return probability. Moreover, equation (24) hides the assumption of isotropy of the distribution function of the accelerated particles, since that formula was conceived in a discussion of nonrelativistic shocks (Peacock [1981] introduced this formalism for particle acceleration at relativistic shock fronts). All these limitations become of particular importance for relativistic shocks. A general expression for the slope was found in Vietri (2003) and reads

$$\langle P_{\rm ret} \rangle \langle G^{s-3} \rangle = 1. \tag{25}$$

In the following we use equation (24), since we only want to provide the reader with an argument of plausibility for the steepening of the spectra in those cases in which particle leakage can take place in the upstream region. In order to account for this leakage, which cannot take place in the standard scenario of diffusive particle acceleration at a shock front, we generalize equation (24) in order to include the probability of escape from the acceleration box from upstream. This is easily achieved by

TABLE 1

EXACT SPECTRAL SLOPE, MEAN AMPLIFICATION, AND DOWNSTREAM RETURN PROBABILITY FOR $\Gamma_s \beta_s = 5.0$

Regime	Slope	$\langle G \rangle$	$\langle P_{\rm ret}^{\rm (down)} \rangle$
SPAS	4.218 ± 0.001	2.0387	0.4165
LAS	4.445 ± 0.001	2.0753	0.3430

NOTE.—Values are as defined in eqs. (26) and (29).

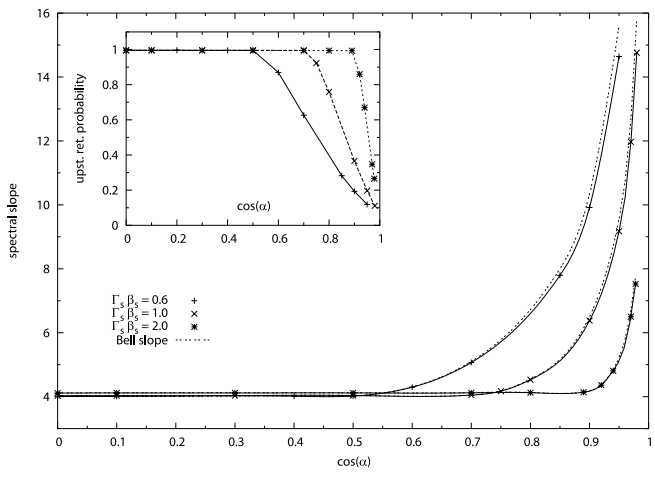

FIG. 8.—Spectral slope as a function of $\cos \alpha$ for three different values of the shock speed. The dashed lines show the spectral slope computed with Bell's method. *Inset*: Corresponding upstream return probabilities.

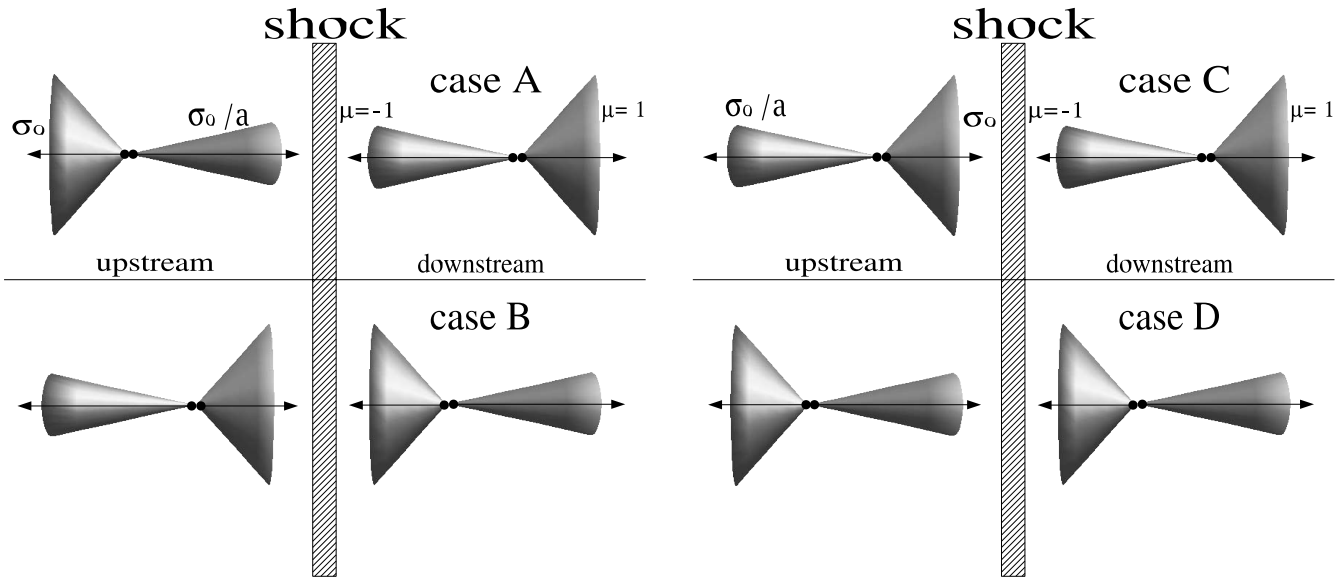

FIG. 9.—Pictorial representation of the four patterns of anisotropic scattering considered in our calculations.

replacing $\langle P_{\rm ret}\rangle$ with $\langle P_{\rm ret}^{\rm (up)}\rangle\langle P_{\rm ret}^{\rm (down)}\rangle$. These mean values expressed in the downstream frame are

$$\left\langle P_{\rm ret}^{\rm (down)}\right\rangle = \frac{\int_{-1}^{-u_d} d\mu_0 \int_{-u_d}^{1} d\mu\, g(\mu)(u_d+\mu)P_d(\mu,\mu_0)}{\int_{-u_d}^{1} d\mu\, g(\mu)(u_d+\mu)}, \quad (26)$$

$$\left\langle P_{\rm ret}^{\rm (up)}\right\rangle = \frac{\int_{-u_d}^{1} d\mu \int_{-1}^{-u_d} d\mu_0\, g(\mu_0)(u_d+\mu_0)P_u(\mu_0,\mu)}{\int_{-1}^{-u_d} d\mu_0\, g(\mu_0)(u_d+\mu_0)}. \quad (27)$$

In the last equation P_u also has to be computed in terms of quantities evaluated in the downstream frame. Energy amplification for a particle entering the upstream region with direction μ_0 (as measured downstream) and returning with direction μ is obtained by combining two Lorentz transformations,

$$G(\mu_0,\mu) = \gamma_{\rm rel}^2(1-u_{\rm rel}\mu_0)(1+u_{\rm rel}\bar{\mu}), \quad (28)$$

where $\bar{\mu} = (\mu + u_{\rm rel})/(1+u_{\rm rel}\mu)$ is the returning direction as seen in the upstream frame. Averaging the amplification, we have

$$\langle G\rangle = \frac{\int_{-1}^{-u} d\mu_0\, g(\mu_0)(u+\mu_0)\int_{-u}^{1} d\mu\, G(\mu_0,\mu)P_u(\mu_0,\mu)}{\int_{-1}^{-u} d\mu_0\, g(\mu_0)(u+\mu_0)\int_{-u}^{1} d\mu\, P_u(\mu_0,\mu)}. \quad (29)$$

The spectral slope as computed through equation (24) is plotted in Figure 8 (*main panel*) with dashed lines; the corresponding upstream return probability $\langle P_{\rm ret}^{\rm (up)}\rangle$ is plotted in the inset (*dashed lines*). The agreement with our exact results is better than 1%, proving that the reason for the softening of the spectra of accelerated particles is in the increased probability that the particles leave the acceleration region when only a large-scale coherent magnetic field is present upstream.

The results discussed above apply to situations in which the magnetic field in the upstream region can be considered as coherent on spatial scales exceeding the size of the acceleration box.

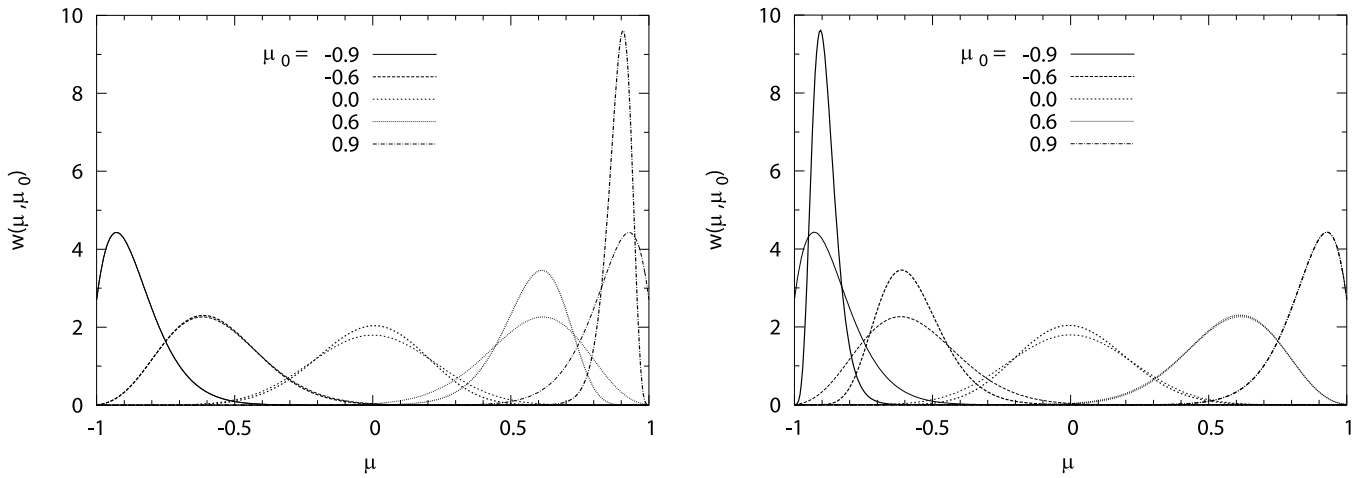

FIG. 10.—Anisotropic scattering functions $w_+(\mu,\mu_0)$ (*left*) and $w_-(\mu,\mu_0)$ (*right*) as functions of μ and for different values of the incoming direction μ_0 are shown by the thick lines. The anisotropy factor is $a = 10$ and $\sigma_0 = 0.05$. For comparison the isotropic scattering function (eq. [10]) is shown with thin lines and for the same values of μ_0.

TABLE 2
SUMMARY OF MEAN SCATTERING ANGLE USED IN THE DIFFERENT SCENARIOS OF FIGURE 9

Location	*A*	*B*	*C*	*D*
Upstream	σ_+	σ_-	σ_-	σ_+
Downstream	σ_-	σ_+	σ_-	σ_+

If the coherence scale of the field is smaller than the size of the accelerator, then the direction of the particles suffer a random wandering motion and one can think of this structured field as the source of diffusion and as a physical mechanism that imposes a maximum energy to the accelerated particles (at least in the absence of radiative energy losses). Particles that escape from the shock region too fast (highest energy ones) have enough time to *feel* the effect of a coherent scale, while lower energy particles live in the accelerator for longer times and in principle may *feel* different orientations of the upstream magnetic field. This scenario is basically equivalent to having some degree of scattering upstream and should be treated with the formalism already discussed in Vietri (2003) and Blasi & Vietri (2005). As soon as a phenomenon equivalent to scattering is present, the probability of escape to upstream infinity vanishes for all those particles that are confined in the accelerator for sufficiently long times. Moreover, one should keep in mind that even if a large-scale coherent magnetic field is present to start with, the propagation of the accelerated (charged) particles in the upstream plasma is very likely to excite fluctuations in the magnetic field structure through streaming instability (Bell 1978). These fluctuations act as scattering centers and enhance the probability of returning to the shock front.

4. ANISOTROPIC SCATTERING

In this section we consider again the standard case in which particle motion in both the upstream and downstream fluids is diffusive due to the presence of scattering agents. However, we include the possibility that the scattering, although spatially constant, may be anisotropic. The physical motivation for this generalization is the following: in a background of Alfvèn waves with a power spectrum $P_W(k)$ [such that $P_W(k)\,dk$ is the energy density in the form of waves with wavenumber in the range dk around k], the particles suffer angular diffusion with a diffusion coefficient

$$D_{\theta\theta} = \left\langle \frac{\Delta\theta\Delta\theta}{\Delta t} \right\rangle \approx \Omega \frac{k_r P_W(k_r)}{B_0^2/8\pi}, \tag{30}$$

where $k_r = \Omega/v\mu$ is the resonant wavenumber and Ω is the gyration frequency of particles with momentum p in the background magnetic field B_0. One can clearly see from equation (30) that the diffusion is anisotropic in general, unless the power spectrum has a specific ad hoc form. One should keep in mind that equation (30) is obtained in the context of quasi-linear theory. A full nonlinear treatment might show how the turbulence is distributed and which is the resulting particle angular distribution.

In the calculations that follow, we quantify the effects of anisotropic scattering on the spectrum and angular distribution of the accelerated particles. The calculation of specific patterns of anisotropy in the scattering agents is beyond the scope of this paper; therefore, we adopt a few simple but physically meaningful toy models of anisotropic scattering, and we carry out the calculations within those models.

4.1. *Modeling Anisotropy*

We parameterize the anisotropy in such a way so as to reproduce the following four patterns:

Case A.—Particles are scattered per unit length more efficiently while they move away from the shock front than they are on their way to the shock front, both upstream and downstream.

Case B (opposite of case *A*).—Particles are scattered per unit length more efficiently on their way to the shock front than they are while they move away from the shock front, both upstream and downstream.

Case C.—In the downstream fluid, particles are scattered per unit length more efficiently while they move away from the shock front ($\mu \to 1$) than they are on their way to the shock front ($\mu \to -1$). In the upstream fluid the situation is reversed, and scattering is more efficient for the particles that are moving toward the shock ($\mu \to 1$).

Case D (opposite of *C*).—Scattering is more effective around $\mu \sim -1$ both upstream and downstream.

A pictorial representation of cases *A*–*D* is shown in Figure 9.

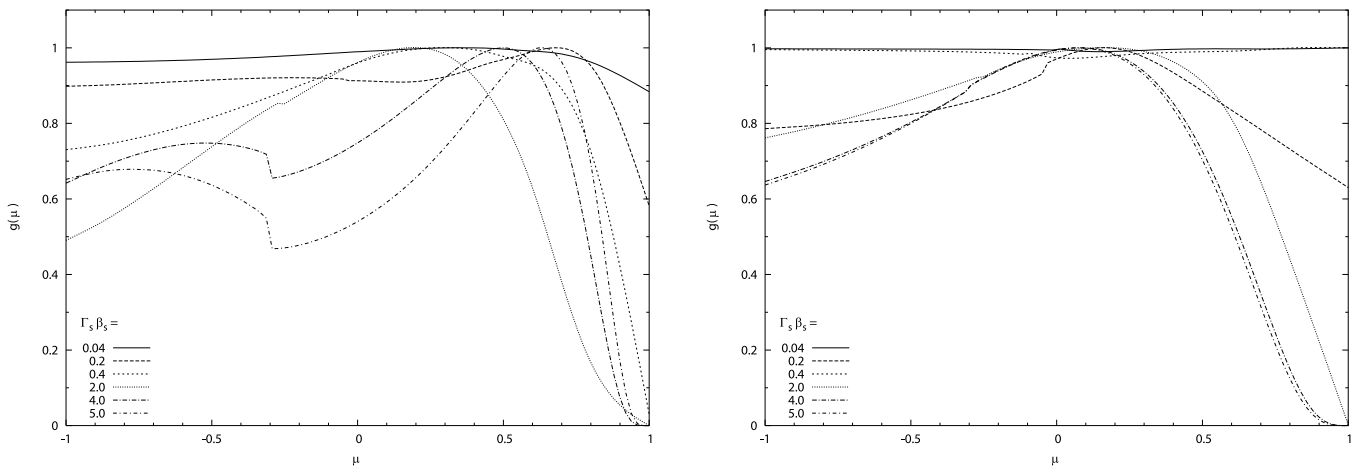

FIG. 11.—Particle distribution function at the shock front for anisotropic scattering of type *A* (*left*) and *B* (*right*), both with $a = 10$. Each line represents a different shock speed as the labels show.

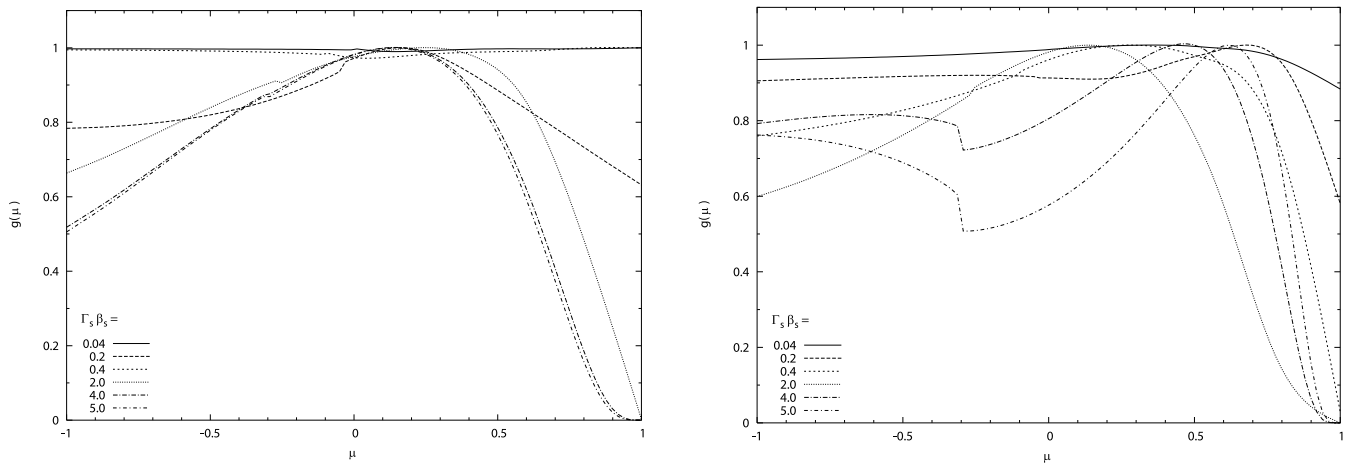

FIG. 12.—Same as Fig. 11, but for anisotropic scattering of type *C* (*left*) and *D* (*right*).

In order to simulate cases *A*–*D* above, we adopt a scattering function similar to equation (10), but modified to introduce anisotropic scattering. In particular, to achieve this goal we allow the width σ of the scattering function to depend on both the initial and final directions μ' and μ, so that

$$w(\mu,\mu') = \frac{1}{\sigma(\mu,\mu')} e^{-[(1-\mu\mu')/\sigma(\mu,\mu')]} \times I_0\left(\frac{\sqrt{1-\mu^2}\sqrt{1-\mu'^2}}{\sigma(\mu,\mu')}\right). \quad (31)$$

It is worth stressing that the scattering function has to be symmetric if we exchange μ with μ', as a consequence of Liouville's theorem, so we are forced to look for a symmetric function $\sigma(\mu,\mu')$. In order to apply the functional form of equation (31) to cases *A*–*D*, it is sufficient to adopt the following expression for the mean scattering angle $\sigma(\mu,\mu')$,

$$\sigma_{\mp}(\mu,\mu') = \sigma_0\left[1 - \frac{(a-1)}{4a}(\mu \mp 1)(\mu' \mp 1)\right]. \quad (32)$$

Both σ_+ and σ_- have σ_0 as the maximum and σ_0/a as the minimum value. For this reason we refer to a as the "anisotropy factor." For $a = 1$ isotropic scattering is recovered.

The resulting scattering function $w_{\mp}(\mu,\mu')$, obtained by substituting equation (32) into equation (31), is plotted in Figure 10 together with the isotropic scattering function (eq. [10]), for $\sigma_0 = 0.05$ and $a = 10$. These plots clarify how w_+ and w_- can simulate a scattering more efficient in the $\mu = 1$ and -1 directions, respectively.

The condition $\int_{-1}^{1} d\mu\, w(\mu,\mu') = 1$, which states the probability conservation, is fulfilled by equation (31) provided $\sigma_0 \ll 1$. In the numerical calculations that follow, we assume $\sigma_0 = 0.05$.

Using σ_- and σ_+ in different combinations for the upstream and the downstream fluids, we can reproduce scenarios *A*, *B*, *C*, and *D*, as summarized in Table 2.

4.2. *Results: Anisotropic Scattering for Shocks of Arbitrary Speed and Fixed Anisotropy Factor*

Following the procedure outlined in § 2 and making use of equations (31) and (32), we compute the spectral index and the angular distribution for scenarios *A*, *B*, *C*, and *D* described above. In each case, both the parameter σ_0 and the anisotropy factor a are fixed ($\sigma_0 = 0.05$ and $a = 10$), while the shock velocity is allowed to vary within the range $0.04 \leq \Gamma_s\beta_s \leq 5$.

The angular part of the distribution function is shown in Figure 11 for scenarios *A* (*left*) and *B* (*right*) and in Figure 12 for scenarios *C* (*left*) and *D* (*right*). The slope of the spectrum of accelerated particles is plotted in Figure 13. For relativistic shocks, the spread in the slope of the spectrum of accelerated particles has less spread around ~4, although in general it remains true that harder spectra are obtained in scenarios *B* and *D*.

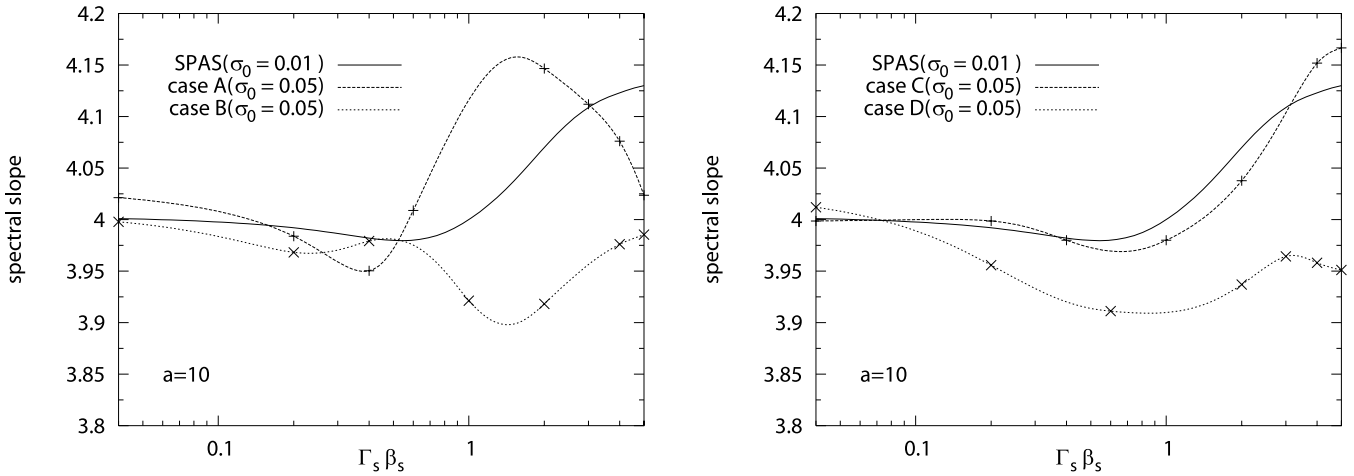

FIG. 13.—Slope vs. shock speed in the four different anisotropic scattering scenarios: *A* and *B* in the left panel, *C* and *D* in the right one. All plots are obtained with $a = 10$ and $\sigma_0 = 0.05$. Slope resulting from isotropic scattering (computed with $\sigma = 0.01$) is also shown for comparison (*solid lines*).

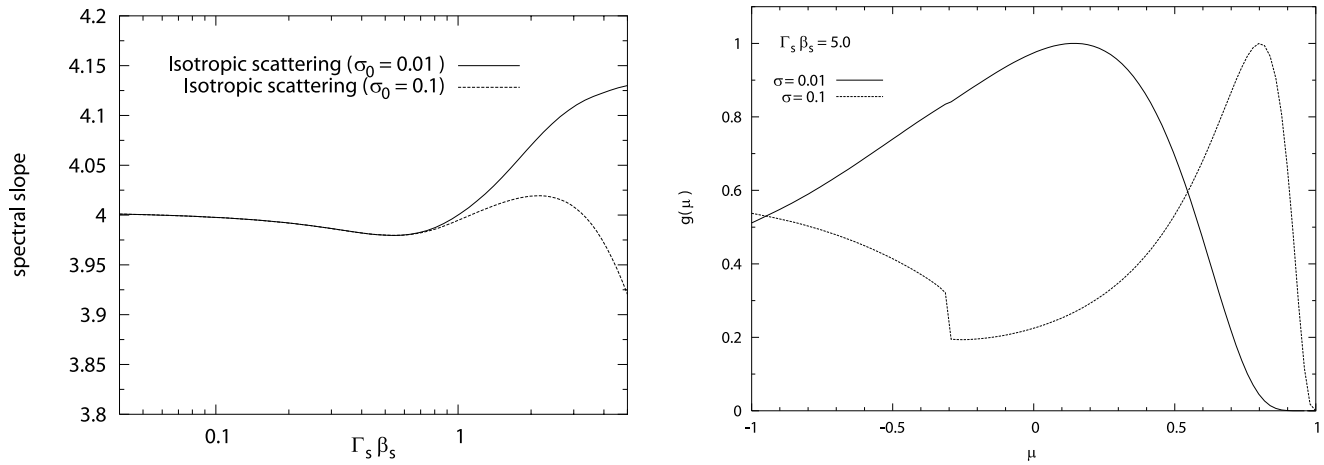

FIG. 14.—Breaking of the SPAS approximation. *Left*: Slope of the spectrum of accelerated particles in the case of isotropic scattering with $\sigma = 0.01$ (*solid line*) and $\sigma = 0.1$ (*dashed line*). *Right*: Angular distribution for $\Gamma_s\beta_s = 5$ with $\sigma = 0.01$ (*solid line*) and $\sigma = 0.1$ (*dashed line*).

A note of caution is necessary to interpret the apparent peak in the slopes at $\Gamma_s\beta_s \sim 1$ for case *A* and at $\Gamma_s\beta_s \sim 3$ for case *D*. These peaks are completely unrelated to anisotropic scattering and are instead the result of the breaking of the regime of small pitch angle scattering (or SPAS), as was already pointed out in Blasi & Vietri (2005). The acceleration process no longer takes place in the SPAS regime when $\Gamma_s^2 \gtrsim 1/4\sigma$, which happens at higher Lorentz factor when σ is smaller. This is shown in Figure 14, where we plot the slope for the case of isotropic SPAS for $\sigma = 0.1$ (*dashed line*) and $\sigma = 0.01$ (*solid line*) and the corresponding angular distribution for $\Gamma_s\beta_s = 5$. As already found in Blasi & Vietri (2005), the transition from SPAS to LAS is generally accompanied by a hardening of the spectra of accelerated particles. The peak seen in Figure 13 is simply the consequence of an effective value of σ in the anisotropic scattering cases *A* and *D*. This is also clear comparing angular distributions of Figure 14 with the angular distribution of cases *A* and *D* for $\Gamma_s\beta_s = 4$ and 5; the curves show the same behavior with a jump at $\mu = -\beta_{\rm down}$ and a peak that moves toward $\mu = 1$ as the shock speed increase.

5. CONCLUSIONS AND DISCUSSION

In this paper we carried out exact calculations of the angular distribution function and spectral slope of the particles accelerated at plane shock fronts moving with arbitrary velocity, generalizing a method previously described in detail in Vietri (2003) and Blasi & Vietri (2005). In particular, we specialized our calculations to two situations: (1) the presence of a large-scale coherent magnetic field of arbitrary orientation with respect to the shock normal, in the upstream fluid, and (2) the possibility of anisotropic scattering in the upstream and downstream plasmas.

Our calculations allowed us to describe the importance of the inclination of the magnetic field when this has a large coherence length and there are no scattering agents upstream. For Newtonian shocks, only quasi-perpendicular fields (namely, perpendicular to the shock normal) are of practical importance, in that the return of particles to the shock from the upstream section is warranted. Quasi-parallel shocks imply a very low probability of return, so that the spectrum of accelerated particles is extremely soft. The process of acceleration eventually shuts off for parallel shocks. For relativistic shocks, the situation is less pessimistic, because the accelerated particles and the shock front move with comparable velocities in the upstream frame. In general, the acceleration stops being efficient when the cosine of the inclination angle α of the magnetic field with respect to the shock normal is comparable with the shock speed in units of the speed of light. The slope of the spectrum of accelerated particles for $\cos\alpha = 0$ as a function of the shock velocity is plotted in Figure 6 for the two cases in which SPAS or LAS is operating in the downstream plasma. The slope as a function of $\cos\alpha = 0$ for shocks moving at different speeds is shown in Figure 8. In the same figure we also show the return probability from the upstream section in order to emphasize that the presence of a large-scale magnetic field upstream leads to particle leakage to upstream infinity. This latter phenomenon disappears when scattering is present, in that scattering always allows for the shock to reach the accelerated particles. In this case, the probability of returning to the shock at an arbitrary direction is unity. One can ask when and how the transition from a situation in which there is no scattering to one in which scattering is at work takes place. When some scattering is present but the energy density in the scattering agents (e.g., Alfvèn waves) is very low compared with the energy density in the background magnetic field, only very low energy particles are effectively scattered. When their energy becomes large enough, they only feel the presence of the coherent field. Increasing the amount of scattering, this transition energy becomes gradually higher. Particles whose Larmor radius is larger than the coherence scale of the magnetic field can eventually escape the accelerator. In general, the level of turbulence (and therefore of scattering) and the number of accelerated particles are not independent, since the turbulence may be self-generated through streaminglike instabilities Bell (1978).

In § 4 we extended our analysis to the very interesting case of anisotropic scattering in both the upstream (unshocked) and downstream (shocked) medium. The pattern of anisotropy, which clearly depends on the details of the formation and development of the scattering centers, has been parameterized in four different scenarios, and for each one we calculated the angular part of the distribution function and the spectrum of the accelerated particles. Deviations from the predictions obtained in the context of isotropic SPAS and LAS have been quantified; the typical magnitude of these deflections is a few percent, but there are situations in which the deviation is more interesting, in particular, because it goes in the direction of making spectra harder.

This research was partially funded through grant COFIN 2004-2005. P. B. is grateful to the KIPAC at SLAC/Stanford for hospitality during the final stages of preparation of the manuscript.

REFERENCES

Achterberg, A., Gallant, Y. A., Kirk, J. G., & Guthmann, A. W. 2001, MNRAS, 328, 393
Bednard, J., & Ostrowski, M. 1998, Phys. Rev. Lett., 80, 3911
Bell, A. R. 1978, MNRAS, 182, 147
Blasi, P., & Vietri, M. 2005, ApJ, 626, 877
Freiling, G., Vietri, M., & Yurko, V. 2003, Lett. Math. Phys., 64, 65
Gallant, Y. A. 2002, in Relativistic Flows in Astrophysics, ed. A. W. Guthmann et al. (Berlin: Springer), 24
Gallant, Y. A., & Achterberg, A. 1999, MNRAS, 305, L6
Kirk, J. G., & Duffy, P. 1999, J. Phys. G, 25, R163
Kirk, J. G., Guthmann, A. W., Gallant, Y. A., & Achterberg, A. 2000, ApJ, 542, 235
Kirk, J. G., & Schneider, P. 1987, ApJ, 315, 425
Lemoine, M., & Pelletier, G. 2003, ApJ, 589, L73
Lemoine, M., & Revenu, B. 2006, MNRAS, 366, 635
Niemiec, J., & Ostrowski, M. 2004, ApJ, 610, 851
Peacock, J. A. 1981, MNRAS, 196, 135
Synge, J. L. 1957, The Relativistic Gas (Amsterdam: North-Holland)
Vietri, M. 2003, ApJ, 591, 954